

Referring Image Matting

Jizhizi Li¹

Jing Zhang¹

Dacheng Tao^{2,1}

¹The University of Sydney, Australia,

²JD Explore Academy, China

jili8515@uni.sydney.edu.au, jing.zhang1@sydney.edu.au, dacheng.tao@gmail.com

Abstract

Image matting refers to extracting the accurate foregrounds in the image. Current automatic methods tend to extract all the salient objects in the image indiscriminately. In this paper, we propose a new task named **Referring Image Matting (RIM)**, referring to extracting the meticulous alpha matte of the specific object that can best match the given natural language description. However, prevalent visual grounding methods are all limited to the segmentation level, probably due to the lack of high-quality datasets for RIM. To fill the gap, we establish the first large-scale challenging dataset **RefMatte** by designing a comprehensive image composition and expression generation engine to produce synthetic images on top of current public high-quality matting foregrounds with flexible logics and re-labelled diverse attributes. RefMatte consists of 230 object categories, 47,500 images, 118,749 expression-region entities, and 474,996 expressions, which can be further extended easily in the future. Besides this, we also construct a real-world test set with manually generated phrase annotations consisting of 100 natural images to further evaluate the generalization of RIM models. We first define the task of RIM in two settings, i.e., prompt-based and expression-based, and then benchmark several representative methods together with specific model designs for image matting. The results provide empirical insights into the limitations of existing methods as well as possible solutions. We believe the new task RIM along with the RefMatte dataset will open new research directions in this area and facilitate future studies. The dataset and code will be made publicly available at <https://github.com/JizhiziLi/RIM>.

1 Introduction

Image matting refers to extracting the soft alpha matte of the foreground in natural images, which is beneficial for various downstream applications such as video conferences, advertisement production, and e-Commerce promotion [49]. Typical matting methods can be divided into two groups: 1) the methods based on auxiliary inputs, e.g., trimap [13; 1], and 2) automatic matting methods that can extract the foreground without any human intervention [15; 16; 14]. However, the former ones are not applicable for automatic application scenarios, and the latter ones are generally limited to specific object categories, e.g., human [2; 48; 26], animal [15], or all the salient objects [50; 33]. It is still unexplored to carry out controllable image matting on arbitrary objects, i.e., extracting the alpha matte of the specific object that can best match the given natural language description.

Language-driven tasks such as referring expression segmentation (RES) [46], referring image segmentation (RIS) [8; 45; 20], visual question answering (VQA) [4], and referring expression comprehension (REC) [24], have been widely explored. Great progress in the areas has been made based on many datasets like ReferIt [10], Google RefExp [27], RefCOCO [47], VGPhraseCut [40], and Cops-Ref [3]. For example, RES methods aim to segment arbitrary object indicated by the natural language description. Nevertheless, the obtained masks are limited to the segmentation level without fine details, due



Figure 1: Some examples from our RefMatte test set (top) and the results of our CLIPMat given prompt and expression input (bottom).



Figure 2: Some examples from our RefMatte-RW100 test set (top) and the results of our CLIPMat given expression input (bottom).

to the low-resolution images and coarse mask annotations in the datasets. Therefore, it is impossible for them to be used in the scenarios that require a meticulous alpha matte of the foreground object.

To fill this gap, we propose a new task named **Referring Image Matting (RIM)** in this paper. RIM refers to extracting the specific foreground object in the image that best matches the given natural language description together with a meticulous high-quality alpha matte. Different from the tasks that were solved by the two kinds above-mentioned matting methods, RIM aims for controllable image matting on arbitrary objects in the image indicated by language description. It is of practical significance in industrial application domains and opens up new research directions in academia community. To facilitate the study of RIM, we establish the first dataset named **RefMatte**, which consists of 230 object categories, 47,500 images, and 118,749 expression-region entities together with the corresponding high-quality alpha mattes and 474,996 expressions. Specifically, to build up this dataset, we first revisit a lot of prevalent public matting datasets like AM-2k [15], P3M-10k [14], AIM-500 [16], SIM [37] and manually label the category of every object (a.k.a. entity) carefully. We also adopt multiple deep learning-based pre-trained models [21; 41] to generate various attributes for each entity, such as gender, age, and clothes type of human. Then, we design a comprehensive composition and expression generation engine to generate the synthetic images with reasonable absolute and relative positions considering other foreground objects. Finally, we present several expression logic forms to generate varying language descriptions by making use of the rich visual attributes. In addition, we propose a real-world test set RefMatte-RW100 with 100 images containing diverse objects and human-annotated expressions, which is used to evaluate the generalization ability of RIM methods. Some examples are shown in Figure 1 and Figure 2.

To provide fair and comprehensive evaluation of the state-of-the-art methods in relevant tasks, we benchmark them on RefMatte under two different settings, i.e., the prompt-based setting and expression-based setting, depending on the form of language descriptions. Since the representative methods are particularly designed for segmentation tasks [23; 9], there are still gaps when directly applying them on the RIM task. To address this issue, we propose two strategies to customize them for RIM, i.e., 1) we carefully design a light-weight matting head on top of CLIPSeg named CLIPMat to generate high-quality alpha matte results while keeping its end-to-end trainable pipeline; and 2) we provide several separate coarse map-based matting methods to serve as post refiners to further improve the segmentation/matting results. Extensive experimental results 1) show the value of the proposed RefMatte dataset for the research of the RIM task, 2) identify the important role of the form of language descriptions; and 3) validate the effectiveness of the proposed customization strategies. Figure 1 and Figure 2 show some results of the proposed CLIPMat given prompt and expression.

The main contribution of this study is three-fold. 1) We define a new task named RIM, aiming at identifying and extracting the alpha matte of the specific foreground object that best matches the

given natural language description; 2) We establish the first large-scale dataset RefMatte, consisting of 47,500 images and 118,749 expression-region entities with high-quality alpha mattes and flowery expressions; 3) We benchmark representative state-of-the-art methods with two customization strategies for RIM on RefMatte under two different settings and gain some useful insights.

2 Related work

Image matting Image matting is a fundamental vision task that is essential for various downstream applications. Previous image matting methods are divided into two groups depending on whether or not they use auxiliary user inputs. In the first group, the methods use a three-class trimap [43; 18], or a background image from the same scene [19], or a coarse map [48] as the auxiliary input to provide guidance for estimating the alpha matte. In the second group, the methods [33; 50; 2; 15; 16; 11; 14] extract the foreground objects automatically without any manual efforts involved. Recently, there are also some works making effort on controlling the matting process by determining which objects can be extracted. For example, Xu et al. propose a matting method [42] to extract the foreground human and all related objects automatically for human-object interaction. Sun et al. propose to extract each foreground human instance separately rather than extracting all of them indiscriminately [38]. However, it is still unexplored for controllable image matting by using natural language description as guidance to extract specific foreground object that best matches the input text, although it is an efficient and flexible way for the matting model to interact with a human. In this paper, we fill this gap by proposing the RIM task, RefMatte dataset, and effective solutions.

Matting datasets Many matting datasets have been proposed to advance the progress in the image matting area. Typical matting datasets contain high-resolution images belonging to some specific object categories that have lots of details like hair, accessories, fur, and net as well as transparent objects. For example, the matting datasets proposed by Xu et al. [43], Qiao et al [33], Sun et al. [37], and Li et al. [16] contain many different categories of objects including human, animal, car, plastic bag and plant. Besides, there are some other matting datasets focusing on a specific category of object, e.g., humans in P3M-10K [14] and animals in AM-2K [15]. In addition to the foreground objects, background images are also useful for generating abundant composite images. For example, Li et al. [15] propose a large-scale background dataset containing 20k high-resolution and diverse background images, which are helpful to reduce the domain gap between composite images and natural images. All the above datasets have open licenses and can be used to further construct customized matting datasets, e.g., the proposed RefMatte dataset.

Vision-language tasks and methods Vision-Language tasks such as RIS [8], RES [46], REC [25], text-driven manipulation [30], and text-to-image generation [32; 31; 35], have been widely explored and are useful for lots of applications like interactive image editing. Among them, RIS aims to segment the target object given language expression is most related to our work. RIS methods can be divided into single-stage ones [20; 17; 23; 39; 36] and two-stage ones [9; 46; 7; 22]. The former ones directly train a segmentation network by leveraging the pre-trained models like CLIP [34], while the latter ones perform region proposal and segmentation sequentially. However, they usually generate low-resolution and coarse object masks due to the task setting (i.e., for segmentation rather than matting) and the lack of high-quality annotations (e.g., alpha mattes) [10; 27; 47; 40]. By contrast, we propose the RIM task along with the RefMatte dataset to facilitate the research of generating alpha matte of the foreground object described by natural language. Moreover, we customize the above RIS methods for RIM, benchmark their performances on RefMatte, and discuss the limitations.

3 The RefMatte dataset

In this section, we present the overview pipeline of constructing RefMatte (Sec. 3.1 and Sec. 3.2) along with the task settings (Sec. 3.3) and statistics of the dataset (Sec. 3.5). Some examples from RefMatte are shown in Figure. 3. Furthermore, we also construct a real-world test set consisting of 100 natural images with manually labelled annotations of flowery language descriptions (Sec. 3.4).

3.1 Preparation of matting entities

To prepare enough high-quality matting entities to help construct our RefMatte dataset, we revisit currently available matting datasets to filter out foregrounds that satisfy our requirements. We then

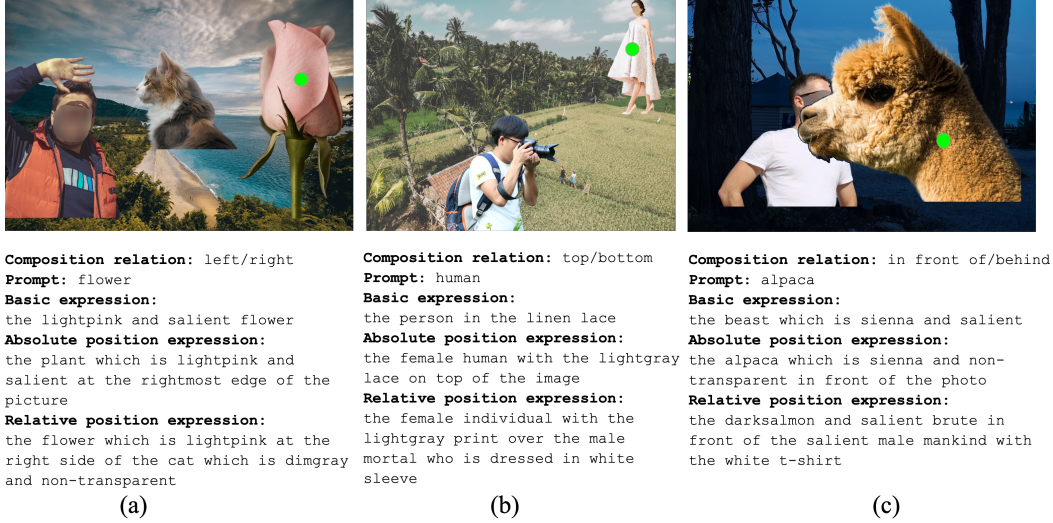


Figure 3: Some examples from our RefMatte dataset. The first row shows the composite images with different foreground instances while the second row shows the natural language descriptions corresponding to the specific foreground instances indicated by the green dots.

manually label the categories for all the candidate entities and annotate their attributes leveraging multiple deep learning-based pre-trained models [21; 41]. We present the details as follows.

Pre-processing and filtering Due to the nature of the image matting task, all the candidate entities should be in high-resolution, with clear and fine details in the alpha matte. Moreover, the data should be publicly available with open licences and without privacy concerns to facilitate future research. With regard to these requirements, we adopt all the foreground images from AM-2k [15], P3M-10k [14], and AIM-500 [16]. Specifically, for P3M-10k, we filter out the images with more than two adhesive foreground instances to make sure each entity is related to only one foreground instance. For other available datasets like SIM [37], DIM [43], and HATT [33], we filter out those foreground images with identifiable faces in human instances. We also filter out those foreground images in low-resolution or having low-quality alpha mattes. The final number of the entities is 13,187 in total, whose details could be found in the supplemental material. For the background images used in the following composition step, we choose all the images in BG-20k [15].

Annotate the category names of entities Since previous automatic matting methods tend to extract out all the salient foreground objects from the image, they do not provide the specific (category) name for each entity. However, for the RIM task, we need the entity name to describe it. Following [29], we label the *entry-level category name* for each entity, which stands for the most common used name for the specific entity by people. Here, we adopt a semi-automatic strategy. Specifically, we use the Mask RCNN detector [5] with a ResNet-50-FPN [6] backbone from [41] to automatically detect and label the category names for each foreground instance and then manually check and correct them. In total, we have 230 categories in RefMatte. Furthermore, we adopt WordNet [28] to generate synonyms for each category name to enhance the diversity. We manually check the synonyms and replace some of them with more reasonable ones. The details are presented in the supplemental material.

Annotate the attributes of entities To ensure all the entities having rich visual properties to support forming abundant expressions, we annotate all entities with several attributes such as color for all entities; gender, age, and clothes type for the human entities. We also adopt a semi-automatic strategy to generate such attributes. For generating color, we cluster all the pixel values of the foreground image, find out the most frequent value, and match it with the specific color in webcolors. For gender and age, we adopt the pre-trained models provided by Levi et al. in [12], and follow the common sense to define the age group based on the predicted ages. For clothes type, we adopt the pre-trained model provided by Liu et al. in [21]. Furthermore, motivated by the categorization of foreground types in [16], we add the attributes of salient or not as well as transparent or not for all entities, since such attributes are also important in the image matting task. In summary, we have at least 3 attributes for each entity and 6 attributes for human entities.

3.2 Image composition and expression generation

Based on the collected matting entities in the previous section, we propose an image composition engine and expression generation engine to construct our RefMatte dataset. How to arrange different entities to form reasonable composite images while generating semantically clear, grammatically correct, abundant and fancy expressions to describe the entities in these composite images is the key of constructing RefMatte, which is also challenging. To this end, we define six types of position relationships for arranging different entities in a composite image and leverage diverse logic forms to produce appropriate expressions. We present the details as follows.

Image composition engine To keep the high resolution of entities while arranging them with reasonable position relationships, we adopt two or three entities for each composite image. We define six types of position relationships as: *left*, *right*, *top*, *bottom*, *in front of*, and *behind*. For each relationship, we generate the foreground images by [13] and composite them with the background image from BG-20k [15] via alpha blending. Specifically, for the relationships of *left*, *right*, *top*, and *bottom*, we ensure there are no occlusions in the foreground instances to preserve their details. For the relationships of *in front of* and *behind*, we simulate occlusions between the foreground instances by adjusting their relative positions. We prepare a bag of candidate words to denote each relationship. The details are provided in the supplemental material. Some examples are shown in Figure 3.

Expression generation engine To provide abundant expressions for the entities in the composite images, we define three types of expressions for each entity from the aspect of different logic forms defined as follows, where $\langle att_i \rangle$ stands for the attribute, $\langle obj_i \rangle$ stands for the category name, and $\langle rel_i \rangle$ stands for the relationship between the reference entity and the related one:

1. **Basic expression** This is the expression that describes the target entity with as many attributes as one can, e.g., the/a $\langle att_0 \rangle \langle att_1 \rangle \dots \langle obj_0 \rangle$ or the/a $\langle obj_0 \rangle$ which/that is $\langle att_0 \rangle \langle att_1 \rangle$, and $\langle att_2 \rangle$. For example, as shown in Figure 3(a), the basic expression for the flower entity is ‘the lightpink and salient flower’;
2. **Absolute position expression** This is the expression that describes the target entity with many attributes and its absolute position in the image, e.g., the/a $\langle att_0 \rangle \langle att_1 \rangle \dots \langle obj_0 \rangle \langle rel_0 \rangle$ the photo/image/picture or the/a $\langle obj_0 \rangle$ which/that is $\langle att_0 \rangle \langle att_1 \rangle \langle rel_0 \rangle$ the photo/image/picture. For example, as shown in Figure 3(a), the absolute position expression for the flower is ‘the plant which is lightpink and salient at the rightmost edge of the picture’;
3. **Relative position expression** This is the expression that describes the target entity with many attributes and its relative position with another entity, e.g., the/a $\langle att_0 \rangle \langle att_1 \rangle \dots \langle obj_0 \rangle \langle rel_0 \rangle$ the/a $\langle att_2 \rangle \langle att_3 \rangle \dots \langle obj_1 \rangle$ or the/a $\langle obj_0 \rangle$ which/that is $\langle att_0 \rangle \langle att_1 \rangle \langle rel_0 \rangle$ the/a $\langle obj_1 \rangle$ which/that is $\langle att_2 \rangle \langle att_3 \rangle$. For example, as shown in Figure 3(a), the relative position expression for the flower is ‘the flower which is lightpink at the right side of the cat which is dimgray and non-transparent’.

3.3 Dataset split and task settings

We have 13,187 matting entities in total and split out 11,799 for constructing the training set and 1,388 for the test set. For the training/test split, we try to keep the original split in the source matting datasets except for putting all the long-tailed categories to the training set. However, the categories for the training set and test set are not balanced since most of the entities belong to the human or animal categories. Specifically, among the 11,799 entities in the training set, there are 9,186 human, 1,800 animals and 813 objects. In the test set with 1,388 entities, there are 977 human, 200 animals and 211 objects. To balance the categories, we duplicate the entities to achieve a ratio of 5:1:1 for human:animal:object. Consequently, we have 10,550 human, 2,110 animals, and 2,110 objects in the training set, and 1,055 human, 211 animals and 211 objects in the test set.

To generate images for RefMatte, we pick 5 human, 1 animal and 1 object from the training or test split as one group and feed them into the image composition engine. For each group in either train or test split, we generate 20 images to form the training set, and 10 images to form the test set. The ratio of *left/right:top/bottom:in front of/behind* relationships is set to 7:2:1. The number of entities in each image is set to 2 or 3. And for the relationships of *front of/behind*, we always choose 2 entities to keep the high resolution of each entity. After this process, we have 42,200 training images and 2,110 test images. To further enhance the diversity for the combination of entities, we randomly choose

entities and relationships from all candidates to form another 2,800 training images and 390 test images. Finally, we have 45,000 composite images in the training set and 2,500 images in the test set.

1. **Prompt-based setting** The text description in this setting is a prompt, which is the entry-level category name of the entity, e.g., the prompt in Figure 3 is *flower*, *human*, and *alpaca*, respectively;
2. **Expression-based setting** The text description in this setting is the generated expression in previous section, chosen from the basic expressions, absolute position expressions, and relative position expressions. Some examples can also be seen from Figure 3.

Since RefMatte is built upon composites images, there may exist a domain gap between them and real-world images. To investigate the generalization ability of RIM models trained on it to real-world images, we further establish a real-world test set name **RefMatte-RW100**, which consists of 100 real-world high-resolution images with 2 to 3 entities in each image. We then annotate their expressions following the same three settings in Sec. 3.2. In addition, we add a free expression to the annotations. For the high-quality alpha matte labels, we generate them using image editing softwares, e.g., Adobe Photoshop and GIMP. Some examples from RefMatte-RW100 are shown in Figure 2.

Dataset	Setting	Split	Images Num.	Mattes Num.	Text Num.	Categories Num.	Attrs. Num.	Rel. Num.	Texts Length.
RefMatte	Prompt	train	30,391	77,849	77,849	230	-	-	1.06
		test	1,602	4,085	4,085	66	-	-	1.04
	Expression	train	45,000	112,506	449,624	230	132	31	16.86
		test	2,500	6,243	24,972	66	102	31	16.80
RefMatte-RW100	Expression	test	100	221	884	29	135	34	12.01

We calculate the statistics of the RefMatte dataset and RefMatte-RW100 test set in Table 1. For the prompt-based setting, since the text description is the entry-level category name, we remove the images with multiple entities belonging to the same category to avoid ambiguous reasoning. Consequently, we have 30,391 images in the training set and 1,602 images in the test set in this setting. The number of alphamattes, text descriptions, categories, attributes, and relationships are shown in the following columns, respectively. The average text length in the prompt-based setting is about 1, since there is usually a single word for each category, while it is much larger in the expression-based setting, i.e., about 16.8 in RefMatte and 12 in RefMatte-RW100.

Figure 4: The wordcloud of the prompts (a), attributes (b), and relationships (c) in RefMatte.

4 Experiments

4.1 Experiment settings

Implementation details Since RIM is a totally new task that has not been explored before, we choose to benchmark state-of-the-art methods from relevant tasks including RIS and RES. Specifically, we benchmark two typical methods CLIPSeg [23] and MDETR [9] that represent two main streams of RIS and RES tasks. We use the code provided by the authors and made slight modifications to customize them for the RIM task as described later. We train them on the RefMatte training set with the weights pre-trained on VGPhraseCut [40]. We resize the image to 512×512 during training. The models are trained on NVIDIA A100 GPUs with the batch size and learning rate set following the original papers. For the expression-based setting, we randomly choose one expression from the three types introduced in Sec. 3.2 during training. During test, we also randomly choose one expression for each image. In addition, we report the performance of different methods per expression type.

Customization strategies Since there is a task discrepancy between RIM and RIS/RES, we find that the results of directly applying RIS/RES methods to RIM are not promising, e.g., the details of alpha mattes are not clear. To address the issue, we propose two strategies to customize them for RIM:

1. **Adding matting head** We design light-weight matting heads on top of existing models to generate high-quality alpha mattes while keeping the end-to-end trainable pipeline. Specifically, we design a light version of the matting decoder in GFM [15] on top of CLIPSeg [23], termed **CLIPMat**;
2. **Using matting refiner** We adopt separate coarse map-based matting methods as the post refiners to further improve the segmentation/matting results of above-mentioned methods. Specifically, we train GFM [15] and P3M [14] with the input of image and coarse map as the matting refiner.

Evaluation metrics Following the common practice in previous matting methods [43; 15; 14], we use the sum of absolute differences (SAD), mean squared error (MSE), and mean absolute difference (MAD) to evaluate the performance of different methods, which are averaged over all the entities in the test set. Moreover, we calculate the average SAD, MSE, and MAD for the entities in each image, and average them over the test set, denoted as SAD-E, MSE-E, MAD-E, respectively.

4.2 Main results

4.2.1 Prompt-based setting

We evaluate MDETR [9], CLIPSeg [23] and CLIPMat on the prompt-based setting of RefMatte test set, and show the quantitative results in Table 2. As can be seen, our customized method CLIPMat performs the best compared with MDETR and CLIPSeg, no matter whether the matting refiners are used or not, validating the effectiveness of adding a matting head to customize CLIPSeg for the RIM task. Besides, using either of the two matting refiners can further improve the performance of the three methods. Specifically, P3M [14] performs slightly better than GFM [15] due to its effective design for promoting interactions between the decoders and the effective encoder [44].

Table 2: Results on the RefMatte test set under the prompt-based setting.

Dataset	Method	Refiner	SAD	MSE	MAD	SAD-E	MSE-E	MAD-E
RefMatte test set	MDETR [9]	-	32.27	0.0137	0.0183	33.52	0.0141	0.0190
		GFM [15]	28.15	0.0126	0.0160	29.09	0.0129	0.0165
		P3M [14]	27.33	0.0123	0.0155	28.22	0.0126	0.0160
	CLIPSeg [23]	-	17.75	0.0064	0.0101	18.69	0.0067	0.0106
		GFM [15]	12.70	0.0045	0.0072	13.34	0.0047	0.0076
		P3M [14]	12.17	0.0042	0.0069	12.75	0.0044	0.0073
	CLIPMat	-	12.95	0.0045	0.0074	13.54	0.0047	0.0077
		GFM [15]	11.45	0.0039	0.0065	11.95	0.0040	0.0068
		P3M [14]	11.05	0.0037	0.0063	11.52	0.0038	0.0066

4.2.2 Expression-based setting

We also evaluate these three methods under the expression-based setting on the RefMatte test set and RefMatte-RW100, and show the quantitative results in Table 3. CLIPMat again performs the

best on the RefMatte test set owing to its good ability to preserve more details. When testing on RefMatte-RW100, single-stage methods like CLIPSeg and CLIPMat fall behind the two-stage one, i.e., MDETR, probably due to the better ability of the detector of MDETR in understanding cross-modal semantics. Nevertheless, it is noteworthy that the results under the expression-based setting are much worse than those on the prompt-based setting in Table 2, implying that it is more difficult to infer the correct foreground entity from the long text sentence. Besides, the results on RefMatte-RW100 are worse than those on RefMatte test set, since there is a domain gap between synthetic images and real-world ones as also shown in [15]. More efforts could be made to reduce the domain gap and improve the generalization ability of RIM models trained on synthetic images.

Table 3: Results on the RefMatte test set and RefMatte-RW100 under the expression-based setting.

Dataset	Method	Refiner	SAD	MSE	MAD	SAD-E	MSE-E	MAD-E
RefMatte test set	MDETR [9]	-	84.70	0.0434	0.0482	90.45	0.0463	0.0515
		GFM [15]	81.65	0.0429	0.0464	87.14	0.0459	0.0496
		P3M [14]	80.48	0.0424	0.0458	85.83	0.0452	0.0488
	CLIPSeg [23]	-	69.13	0.0358	0.0394	73.53	0.0381	0.0419
		GFM [15]	64.80	0.0343	0.0369	68.94	0.0365	0.0393
		P3M [14]	64.48	0.0341	0.0367	68.56	0.0364	0.0391
	CLIPMat	-	57.08	0.0296	0.0323	60.76	0.0315	0.0344
		GFM [15]	55.67	0.0290	0.0315	59.28	0.0310	0.0336
		P3M [14]	55.38	0.0289	0.0313	58.97	0.0308	0.0334
RefMatte-RW100	MDETR [9]	-	131.58	0.0675	0.0751	136.59	0.0700	0.0779
		GFM [15]	127.25	0.0673	0.0725	132.26	0.0699	0.0753
		P3M [14]	125.78	0.0669	0.0717	130.72	0.0697	0.0744
	CLIPSeg [23]	-	211.86	0.1178	0.1222	222.37	0.1236	0.1282
		GFM [15]	207.49	0.1171	0.1198	217.26	0.1226	0.1254
		P3M [14]	207.04	0.1166	0.1195	216.93	0.1222	0.1252
	CLIPMat	-	219.06	0.1228	0.1255	225.53	0.1265	0.1293
		GFM [15]	217.88	0.1220	0.1248	224.39	0.1257	0.1286
		P3M [14]	220.17	0.1232	0.1261	226.36	0.1268	0.1297

4.2.3 Impact of input texts

Impact of prompt templates To investigate the impact of the input forms of prompts, we evaluate the performance of different prompt templates. In addition to the traditional template used in [34], we add more templates that are specifically designed for the image matting task, e.g., the foreground/mask/alpha matte of <entity name>. The results are shown in Table 4. We can see that the performance of CLIPMat given different prompts varies a lot, where the basic <entity name> template delivers the best result while the mask of <entity name> leads to the worst. We suspect it is because other forms of prompts beyond <entity name> have not been seen during training. More efforts on prompt augmentation could be explored in future work.

Impact of different expressions Since we have introduced different types of expressions in our task, it is interesting to see the influence of each type on the matting performance. As shown in Table 5, we test the best performed model CLIPMat on the RefMatte test set and the model MDETR on RefMatte-RW100. As can be seen, the absolute position expression is more informative (or easy to understand) than others, leading to the best-performance on both the synthetic test set as well as the real-world one. The performance could be degraded by about 2 or 4 times when using the relative position expression, probably due to the fact that it is more difficult to identify the correct entity when many attributes words and the name of other entities are involved in the expression. Besides, the free expressions which are labeled by human annotators following their preferred style, lead to the worst results, mainly due to the significant diversity of logic, grammar, and words used to describe the entities. More efforts could be made to study the most effective expressions that matter in automatic applications as well as improving the generalization ability of RIM models to deal with diverse expressions in human-machine interaction applications.

5 Limitation and discussion

Based on RefMatte, we benchmark representative methods for the RIM task and obtain useful empirical insights. Despite the large scale of RefMatte and the effectiveness of the proposed baseline

Table 4: Results of CLIPMat with different prompt templates on the RefMatte test set under the prompt-based setting. <en>: <entity name>.

prompt template	SAD	MSE	MAD
<en>	12.95	0.0045	0.0074
a photo of a <en>	13.87	0.0050	0.0079
a photograph of a <en>	14.58	0.0054	0.0083
an image of a <en>	13.69	0.0049	0.0078
the foreground of the <en>	18.16	0.0075	0.0104
the mask of the <en>	53.28	0.02699	0.0305
the alpha matte of the <en>	22.77	0.0102	0.0131
to extract the <en>	14.04	0.0050	0.0080

Table 5: Expression-based RIM results on RefMatte and RefMatte-RW100. BE: basic expression. APE: absolute position expression. RPE: relative position expression. FE: free expression.

Dataset	Expression	SAD	MSE	MAD
RefMatte test set	BE	64.83	0.0341	0.0368
	APE	17.49	0.0074	0.0100
	RPE	81.40	0.0432	0.0461
RefMatte -RW100	BE	114.39	0.0058	0.0065
	APE	72.58	0.0355	0.0417
	RPE	135.97	0.0698	0.0774
	FE	144.80	0.0748	0.0828

model CLIPMat and post refinement strategy, there are still rooms for improvement. First, more effective end-to-end single-stage model could be further studied since two-stage methods may suffer from the wrong predictions in the first stage as demonstrated in previous matting works [15; 14]. Second, it also matters to reduce the synthetic-to-real domain gap like RSSN in [15] to improve the generalization of RIM models trained on synthetic images. Third, More efforts could be made to improve the cross-modal understanding ability to deal with complex and diverse expressions.

6 Conclusion

In this paper, we propose a novel task named referring image matting (RIM) and establish a large-scale dataset RefMatte. We customize existing representative methods in relevant tasks for RIM and benchmark their performance through extensive experiments on RefMatte. The results provide useful insights on model design, impact of text descriptions, and domain gap between synthetic and real images. We hope that the RefMatte dataset could serve as a test bed to facilitate future study.

Social impact The study of RIM can benefit many practical applications such as interactive image editing and human-machine interaction. RefMatte could facilitate the research in this area. However, the synthetic-to-real domain gap may lead to limited generalization to real-world images. Besides, specific attention should be paid to fairness and privacy-preserving during annotating the expressions.

References

- [1] S. Cai, X. Zhang, H. Fan, H. Huang, J. Liu, J. Liu, J. Liu, J. Wang, and J. Sun. Disentangled image matting. In *Proceedings of the IEEE International Conference on Computer Vision*, pages 8819–8828, 2019.
- [2] Q. Chen, T. Ge, Y. Xu, Z. Zhang, X. Yang, and K. Gai. Semantic human matting. In *Proceedings of the ACM International Conference on Multimedia*, pages 618–626, 2018.
- [3] Z. Chen, P. Wang, L. Ma, K.-Y. K. Wong, and Q. Wu. Cops-ref: A new dataset and task on compositional referring expression comprehension. *2020 IEEE/CVF Conference on Computer Vision and Pattern Recognition (CVPR)*, pages 10083–10092, 2020.
- [4] C. Gan, Y. Li, H. Li, C. Sun, and B. Gong. Vqs: Linking segmentations to questions and answers for supervised attention in vqa and question-focused semantic segmentation. In *Proceedings of the IEEE international conference on computer vision*, pages 1811–1820, 2017.
- [5] K. He, G. Gkioxari, P. Dollár, and R. Girshick. Mask r-cnn. In *Proceedings of the IEEE international conference on computer vision*, pages 2961–2969, 2017.
- [6] K. He, X. Zhang, S. Ren, and J. Sun. Deep residual learning for image recognition. In *Proceedings of the IEEE Conference on Computer Vision and Pattern Recognition*, pages 770–778, 2016.
- [7] R. Hu, M. Rohrbach, J. Andreas, T. Darrell, and K. Saenko. Modeling relationships in referential expressions with compositional modular networks. *2017 IEEE Conference on Computer Vision and Pattern Recognition (CVPR)*, pages 4418–4427, 2017.
- [8] S. Huang, T. Hui, S. Liu, G. Li, Y. Wei, J. Han, L. Liu, and B. Li. Referring image segmentation via cross-modal progressive comprehension. *2020 IEEE/CVF Conference on Computer Vision and Pattern Recognition (CVPR)*, pages 10485–10494, 2020.
- [9] A. Kamath, M. Singh, Y. LeCun, G. Synnaeve, I. Misra, and N. Carion. Mdetr-modulated detection for end-to-end multi-modal understanding. In *Proceedings of the IEEE/CVF International Conference on Computer Vision*, pages 1780–1790, 2021.
- [10] S. Kazemzadeh, V. Ordonez, M. Matten, and T. Berg. Referitgame: Referring to objects in photographs of natural scenes. In *Proceedings of the 2014 conference on empirical methods in natural language processing (EMNLP)*, pages 787–798, 2014.
- [11] Z. Ke, J. Sun, K. Li, Q. Yan, and R. W. Lau. Modnet: Real-time trimap-free portrait matting via objective decomposition. In *AAAI*, 2022.
- [12] G. Levi and T. Hassner. Age and gender classification using convolutional neural networks. *2015 IEEE Conference on Computer Vision and Pattern Recognition Workshops (CVPRW)*, pages 34–42, 2015.
- [13] A. Levin, D. Lischinski, and Y. Weiss. A closed-form solution to natural image matting. *IEEE Transactions on Pattern Analysis and Machine Intelligence*, 30(2):228–242, 2007.
- [14] J. Li, S. Ma, J. Zhang, and D. Tao. Privacy-preserving portrait matting. In *Proceedings of the 29th ACM International Conference on Multimedia*, pages 3501–3509, 2021.
- [15] J. Li, J. Zhang, S. J. Maybank, and D. Tao. Bridging composite and real: towards end-to-end deep image matting. *International Journal of Computer Vision*, pages 1–21, 2022.
- [16] J. Li, J. Zhang, and D. Tao. Deep automatic natural image matting. In Z.-H. Zhou, editor, *Proceedings of the Thirtieth International Joint Conference on Artificial Intelligence, IJCAI-21*, pages 800–806. International Joint Conferences on Artificial Intelligence Organization, 8 2021. Main Track.
- [17] R. Li, K. Li, Y.-C. Kuo, M. Shu, X. Qi, X. Shen, and J. Jia. Referring image segmentation via recurrent refinement networks. *2018 IEEE/CVF Conference on Computer Vision and Pattern Recognition*, pages 5745–5753, 2018.
- [18] Y. Li and H. Lu. Natural image matting via guided contextual attention. In *Proceedings of the AAAI Conference on Artificial Intelligence*, volume 34, pages 11450–11457, 2020.
- [19] S. Lin, A. Ryabtsev, S. Sengupta, B. Curless, S. Seitz, and I. Kemelmacher-Shlizerman. Real-time high-resolution background matting. *arXiv preprint arXiv:2012.07810*, 2020.
- [20] C. Liu, Z. L. Lin, X. Shen, J. Yang, X. Lu, and A. L. Yuille. Recurrent multimodal interaction for referring image segmentation. *2017 IEEE International Conference on Computer Vision (ICCV)*, pages 1280–1289, 2017.
- [21] X. Liu, J. Li, J. Wang, and Z. Liu. Mmfashion: An open-source toolbox for visual fashion analysis. In *ACM Multimedia 2021, Open Source Software Competition*, 2021.
- [22] X. Liu, Z. Wang, J. Shao, X. Wang, and H. Li. Improving referring expression grounding with cross-modal attention-guided erasing. *2019 IEEE/CVF Conference on Computer Vision and Pattern Recognition (CVPR)*, pages 1950–1959, 2019.
- [23] T. Lüddecke and A. S. Ecker. Prompt-based multi-modal image segmentation. *arXiv preprint arXiv:2112.10003*, 2021.
- [24] G. Luo, Y. Zhou, X. Sun, L. Cao, C. Wu, C. Deng, and R. Ji. Multi-task collaborative network for joint referring expression comprehension and segmentation. In *Proceedings of the IEEE/CVF Conference on computer vision and pattern recognition*, pages 10034–10043, 2020.
- [25] G. Luo, Y. Zhou, X. Sun, L. Cao, C. Wu, C. Deng, and R. Ji. Multi-task collaborative network for joint referring expression comprehension and segmentation. *2020 IEEE/CVF Conference on Computer Vision and Pattern Recognition (CVPR)*, pages 10031–10040, 2020.
- [26] S. Ma, J. Li, J. Zhang, H. Zhang, and D. Tao. Rethinking portrait matting with privacy preserving. *arXiv preprint arXiv:2203.16828*, 2022.
- [27] J. Mao, J. Huang, A. Toshev, O. Camburu, A. L. Yuille, and K. Murphy. Generation and comprehension of unambiguous object descriptions. In *Proceedings of the IEEE conference on computer vision and pattern*

- recognition, pages 11–20, 2016.
- [28] G. A. Miller. Wordnet: A lexical database for english. *Commun. ACM*, 38:39–41, 1992.
 - [29] V. Ordonez, J. Deng, Y. Choi, A. C. Berg, and T. L. Berg. From large scale image categorization to entry-level categories. *2013 IEEE International Conference on Computer Vision*, pages 2768–2775, 2013.
 - [30] O. Patashnik, Z. Wu, E. Shechtman, D. Cohen-Or, and D. Lischinski. Styleclip: Text-driven manipulation of stylegan imagery. *2021 IEEE/CVF International Conference on Computer Vision (ICCV)*, pages 2065–2074, 2021.
 - [31] T. Qiao, J. Zhang, D. Xu, and D. Tao. Learn, imagine and create: Text-to-image generation from prior knowledge. In *NeurIPS*, 2019.
 - [32] T. Qiao, J. Zhang, D. Xu, and D. Tao. Mirrorgan: Learning text-to-image generation by redescription. In *Proceedings of the IEEE/CVF Conference on Computer Vision and Pattern Recognition*, pages 1505–1514, 2019.
 - [33] Y. Qiao, Y. Liu, X. Yang, D. Zhou, M. Xu, Q. Zhang, and X. Wei. Attention-guided hierarchical structure aggregation for image matting. In *Proceedings of the IEEE Conference on Computer Vision and Pattern Recognition*, 2020.
 - [34] A. Radford, J. W. Kim, C. Hallacy, A. Ramesh, G. Goh, S. Agarwal, G. Sastry, A. Askell, P. Mishkin, J. Clark, G. Krueger, and I. Sutskever. Learning transferable visual models from natural language supervision. In *ICML*, 2021.
 - [35] A. Ramesh, M. Pavlov, G. Goh, S. Gray, C. Voss, A. Radford, M. Chen, and I. Sutskever. Zero-shot text-to-image generation. *ArXiv*, abs/2102.12092, 2021.
 - [36] Y. Rao, W. Zhao, G. Chen, Y. Tang, Z. Zhu, G. Huang, J. Zhou, and J. Lu. Denseclip: Language-guided dense prediction with context-aware prompting. *ArXiv*, abs/2112.01518, 2021.
 - [37] Y. Sun, C.-K. Tang, and Y.-W. Tai. Semantic image matting. In *Proceedings of the IEEE/CVF Conference on Computer Vision and Pattern Recognition*, pages 11120–11129, 2021.
 - [38] Y. Sun, C.-K. Tang, and Y.-W. Tai. Human instance matting via mutual guidance and multi-instance refinement. *arXiv preprint arXiv:2205.10767*, 2022.
 - [39] Z. Wang, Y. Lu, Q. Li, X. Tao, Y. Guo, M. Gong, and T. Liu. Cris: Clip-driven referring image segmentation. *arXiv preprint arXiv:2111.15174*, 2021.
 - [40] C. Wu, Z. Lin, S. Cohen, T. Bui, and S. Maji. Phrasecut: Language-based image segmentation in the wild. In *Proceedings of the IEEE/CVF Conference on Computer Vision and Pattern Recognition*, pages 10216–10225, 2020.
 - [41] Y. Wu, A. Kirillov, F. Massa, W.-Y. Lo, and R. Girshick. Detectron2. <https://github.com/facebookresearch/detectron2>, 2019.
 - [42] B. Xu, H. Huang, C. Lu, Z. Li, and Y. Guo. Virtual multi-modality self-supervised foreground matting for human-object interaction. In *Proceedings of the IEEE/CVF International Conference on Computer Vision*, pages 438–447, 2021.
 - [43] N. Xu, B. Price, S. Cohen, and T. Huang. Deep image matting. In *Proceedings of the IEEE Conference on Computer Vision and Pattern Recognition*, pages 2970–2979, 2017.
 - [44] Y. Xu, Q. Zhang, J. Zhang, and D. Tao. Vitae: Vision transformer advanced by exploring intrinsic inductive bias. In *NeurIPS*, 2021.
 - [45] L. Ye, M. Rochan, Z. Liu, and Y. Wang. Cross-modal self-attention network for referring image segmentation. *2019 IEEE/CVF Conference on Computer Vision and Pattern Recognition (CVPR)*, pages 10494–10503, 2019.
 - [46] L. Yu, Z. Lin, X. Shen, J. Yang, X. Lu, M. Bansal, and T. L. Berg. Mattnet: Modular attention network for referring expression comprehension. In *Proceedings of the IEEE Conference on Computer Vision and Pattern Recognition*, pages 1307–1315, 2018.
 - [47] L. Yu, P. Poirson, S. Yang, A. C. Berg, and T. L. Berg. Modeling context in referring expressions. In *European Conference on Computer Vision*, pages 69–85. Springer, 2016.
 - [48] Q. Yu, J. Zhang, H. Zhang, Y. Wang, Z. Lin, N. Xu, Y. Bai, and A. Yuille. Mask guided matting via progressive refinement network. In *Proceedings of the IEEE/CVF Conference on Computer Vision and Pattern Recognition (CVPR)*, pages 1154–1163, June 2021.
 - [49] J. Zhang and D. Tao. Empowering things with intelligence: a survey of the progress, challenges, and opportunities in artificial intelligence of things. *IEEE Internet of Things Journal*, 8(10):7789–7817, 2020.
 - [50] Y. Zhang, L. Gong, L. Fan, P. Ren, Q. Huang, H. Bao, and W. Xu. A late fusion cnn for digital matting. In *Proceedings of the IEEE Conference on Computer Vision and Pattern Recognition*, pages 7469–7478, 2019.